Fuel 324 (2022) 124719

Contents lists available at ScienceDirect

Fuel

journal homepage: www.elsevier.com/locate/fuel

Full Length Article

Experimental study on the effects of reheat temperatures on the ammonium bisulfate and ash blend deposition

Yuguo Ni, Yan Rong, Xinfeng Yu, Shengyao Huang, Xue Xue, Hao Zhou *

Zhejiang University, State Key Laboratory of Clean Energy Utilization, Institute for Thermal Power Engineering, Hangzhou 310027, PR China

ARTICLE INFO

Keywords:
Ash deposition
Ammonium bisulfate
Reheat temperature
Self-reheating probe

ABSTRACT

Ammonium bisulfate (ABS) and ash blend deposition blocks and corrodes air preheaters in coal-fired power plants, seriously affecting the safe operation of the boiler, especially when the selective catalytic reduction (SCR) system is widely used. In this work, a self-reheating probe was used to investigate the effects of reheat temperatures on ash deposition cleaning. The results showed that reheating could significantly reduce the ash deposition. When the reheat temperature exceeded 365 °C, the metal surface of the probe could be clearly seen. After ash deposition, the stable relative heat flux was about 0.881, and it increased significantly after reheating. For cases 4 (365 °C), 5 (385 °C) and 6 (430 °C), the relative heat flux after reheating was 0.986, 0.997 and 0.997, respectively. Microstructure results showed that the phenomenon of particle agglomeration was obviously reduced after reheating. X-ray diffraction (XRD) and thermal gravimetric analyzer (TGA) results indicated that the contents of ABS and Ammonium sulfate (AS) were significantly reduced in case 4, and they hardly existed in cases 5 and 6. This work provides a new method for cleaning ash deposition, which has a guiding role in the safe operation of the air preheater.

1. Introduction

More and more clean energy has been developed to reduce carbon dioxide emissions and protect the environment, such as biomass energy [1,2], hydrogen energy [3,4] and solar energy. The Chinese government has also made great efforts to transform or shut down coal-fired units while developing clean energy. However, due to the large base of coal-fired units, coal-fired power generation is still China's primary method. The safe and efficient operation of the units is essential. Nitrogen oxide (NOx) is a major pollutant produced during the combustion process in coal-fired power plants. It can cause photochemical smog, acid rain and other hazards to humans and the environment. Coal-fired power plants generally use selective catalytic reduction (SCR) technology for denitrification to reduce NOx emissions.

The reaction formulas [5] are as follows:

$$4NO + 4NH_3 + O_2 \rightarrow 4\ N_2 + 6H_2O \quad (1)$$

$$NO + NO_2 + 2NH_3 \rightarrow 2\ N_2 + 3H_2O \quad (2)$$

$$2NO_2 + 4NH_3 + O_2 \rightarrow 3\ N_2 + 6H_2O \quad (3)$$

The SCR system will oxidize part of SO_2 to SO_3 while reducing NOx. About 0.6–2.4% of SO_2 in the flue gas will be oxidized to SO_3 [5,6]. Due to catalyst aging, catalyst poisoning and temperature changes in the SCR system, the NH_3 injected during NOx reduction will escape. The SO_3 will react with H_2O and escaped NH_3 in the boiler tail flue to produce ammonium bisulfate (NH_4HSO_4, ABS) and ammonium sulfate ($(NH_4)_2SO_4$, AS). The reaction formulas [5–7] are as follows:

$$SO_3 + NH_3 + H_2O \rightarrow NH_4HSO_4 \quad (4)$$

$$NH_3 + NH_4HSO_4 \rightarrow (NH_4)_2SO_4 \quad (5)$$

$$SO_3 + 2NH_3 + H2O \rightarrow (NH_4)_2SO_4 \quad (6)$$

$$SO_3 + H_2O \rightarrow H_2SO_4 \quad (7)$$

$$NH_3 + H_2SO_4 \rightarrow NH_4HSO_4 \quad (8)$$

$(NH_4)_2SO_4$ is a kind of dry powder with low viscosity. It can be cleaned easily with a soot blower and will not contaminate the heating surface. However, NH_4HSO_4 has strong hygroscopicity and viscosity, which can adsorb fly ash and deposit on the low-temperature heating surface, especially on the air preheater, forming ash deposition, causing the air preheater blockage and corrosion [8].

Researchers have done much research on the formation mechanism

* Corresponding author.
E-mail address: zhouhao@zju.edu.cn (H. Zhou).

https://doi.org/10.1016/j.fuel.2022.124719
Received 31 March 2022; Received in revised form 23 May 2022; Accepted 28 May 2022
Available online 4 June 2022

of ABS and found that the formation of ABS in flue gas is mainly affected by NH_3, SO_3, H_2SO_4 concentration and flue gas temperature. Wright et al. [9] studied the relationship between NH_3 and SO_3 concentrations and ABS formation. Based on the previous work of other researchers and experimental data, Muzio et al. [10] proposed a temperature formula for ABS formation, which is vital for the temperature set of SCR system. Menasha et al. [11,12] studied the physical and chemical properties of ABS deeply, and found that ABS melts at 147 °C, remains in liquid form from 147 °C to 320 °C, and begins to decompose when the temperature exceeds 345 °C. Zhou et al. [13] studied the decomposition of AS and ABS mixture with Fe_2O_3 as a catalyst and gave the chemical reaction formula during decomposition. They found that when the temperature exceeds 500 °C, NH_4^+ is wholly converted into NH_3, and when the temperature exceeds 800 °C, AS and ABS entirely decompose. Li et al. [14] studied the decomposition behavior of NH_4HSO_4 deposited on different cokes in a TG-MS system. They found that NH_3 and H_2SO_4 appear at about 170~223 °C, and H_2SO_4/SO_4^{2-} is reduced to SO_2 by coke when the temperature exceeds 223 °C. Zhu et al. [15] investigated the decomposition of ABS under different catalytic conditions and found that pure ABS begins to decompose at 390 °C and reaches the highest decomposition rate at 490 °C. Coke can promote the decomposition of ABS, and V_2O_5 plays an inhibitory role. Vuthaluru et al. [16] found that sulfate acts as a cementing agent and causes ash aggregation in depositions. At the same time, they pointed out that the severe temperature fluctuation characteristic of the air preheater is an important reason for the formation of depositions. Thermogravimetric analysis of the ash from the air preheater by Wang et al. [8] revealed that the ammonium salts in the ash are primarily ABS, AS, and tschermigite.

For ash deposition removal, current research focuses on reducing deposition formation. Srivastava et al. [17] introduced that injecting alkaline additives into the boiler together with fuel can remove up to 80% of SO_3, and injecting alkaline additives into the tail flue can reduce up to 90% of SO_3. However, this method will increase the concentration of particulate matter in the system. Zhang et al. [18] took $NaHCO_3$ and Na_2CO_3 as removers to remove ABS and found that both removers have removal effects on ABS, while Na_2CO_3 has a better effect.

Adding alkaline additives can effectively reduce the ABS in the flue gas. Nevertheless, this method is not thorough, and there will still be ABS and ash blend deposition on the air preheater after long-term operation. Moreover, it has little effect on the ash deposition formed on the air preheater, even with soot blowers. This work developed a new method for cleaning ABS and ash blend deposition. The experiment used a new self-reheating deposition probe to collect ash deposition. After the deposition was deposited, the deposition surface was heated to reheat temperature to remove the ash deposition. The temperature corresponding to the best cleaning effect was found by changing the reheat temperature. In addition, microscopic morphology, mineral composition and thermal gravimetric were applied to explain the reheating mechanism to remove ash deposition. This work can guide air preheater design and ash deposition removal.

2. Experimental details

2.1. Experimental system

Fig. 1 displays a schematic diagram of the experimental system. It is mainly composed of a flue gas system, a deposition probe system, an exhaust gas cleaning system, and a data acquisition system. A hot-air blower could provide high-temperature air, and ash was stably and continuously added into the flue gas pipeline through the ash feeder to simulate the flue gas atmosphere in the boiler tail flue. Electric tracing band and asbestos heat insulation material were wrapped around the flue gas pipeline to maintain the flue gas temperature stable. The flue gas passed through the "+" type quartz tube, and after being cooled by the quench system, it was introduced into the dust collector by the induced draft fan. At the same time, the induced draft fan also played a role in maintaining the negative pressure of the experimental system. The deposition probe system was used for the deposition of ash. During the test, the probe head extended into the center of the quartz tube, and the fly ash in the flue gas would deposit on the probe head. The probe was cooled by compressed air, and the probe controller controlled the cooling and reheating of the probe head. The specific structure of the probe will be introduced later. The data acquisition system monitored and recorded the temperature data of thermocouples in the probe head in real-time, and the data was stored in the computer.

2.2. Deposition sampling technology

Fig. 2 shows a schematic of the deposition probe and the cross-section of the probe head. The probe is made of stainless steel and is

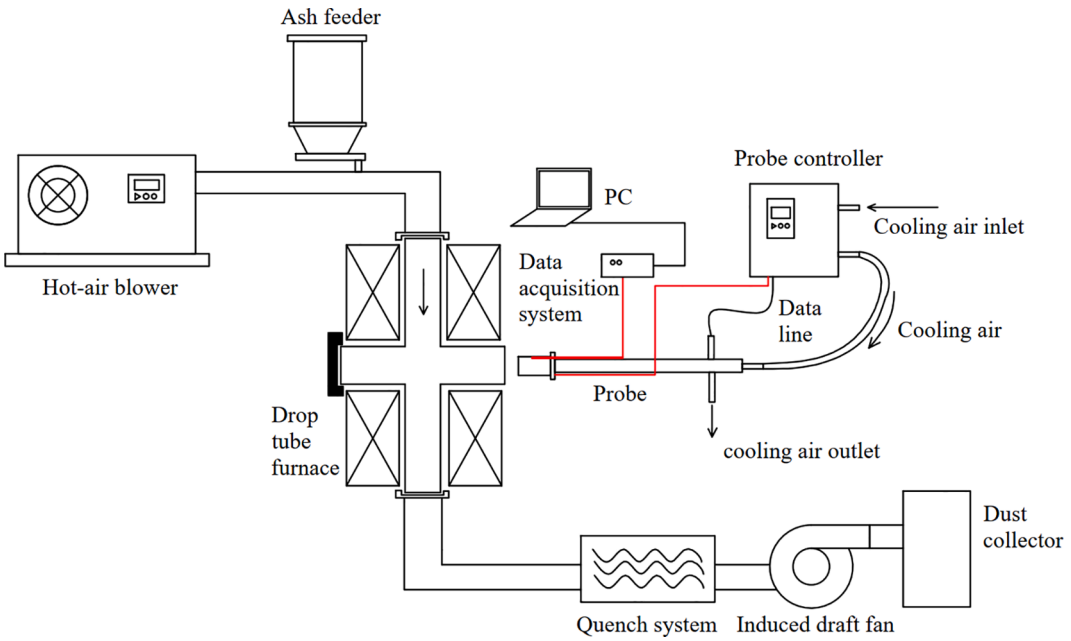

Fig. 1. Schematic diagram of the experimental system.

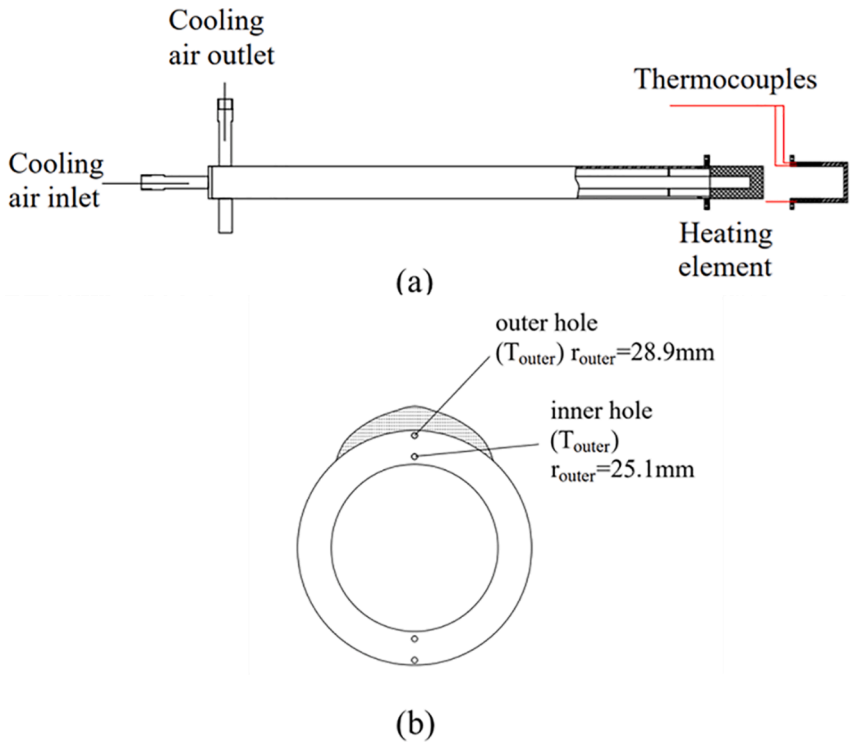

Fig. 2. (a) Schematic of the deposition probe, (b) cross-section of the probe head.

divided into a probe rod and a probe head. The probe head was the ash deposition site and was equipped with a heating element made of silicon carbide material inside, which could heat the surface of the probe head. The compressed air cooled the probe head through the channel in the probe rod. A programmable probe controller controlled cooling and heating. It could set the temperature and holding time of cooling and heating. Two small holes were drilled at the top and bottom of the probe head, just the size to insert into a K-type thermocouple. The distance between the inner hole and the circle's center was 25.1 mm, while the outer hole was 28.9 mm. Two thermocouples were inserted into the upper surface to measure the temperature of the inner and outer holes. And one thermocouple was inserted into the outer hole of the lower surface for the temperature feedback of the probe controller. So the heat flux could be obtained by calculating the temperature difference between the inner and outer holes in the top of the probe by Eq. (9).

$$q = \frac{\lambda(T_{outer} - T_{inner})}{R\ln(\frac{r_{outer}}{r_{inner}})} \quad (9)$$

where q indicates the heat flux through the probe; λ represents the thermal conductivity of the probe material; T_{outer} and T_{inner} denote the temperature of outer and inner holes, respectively; r_{outer} denotes the distance between the outer hole and the center of the circle, $r_{outer} = 28.9$ mm; r_{inner} denotes the distance between the inner hole and the center of the circle, $r_{inner} = 25.1$ mm. R denotes the radius of the probe head, $R = 30$ mm.

2.3. Experimental conditions

Table 1 shows the experimental conditions. This work was focused on the effects of reheat temperatures on ash deposition after the ABS had already formed. It would be difficult to control the ABS concentration if the ABS was generated by NH_3 and SO_3. To directly study the effect of reheat temperatures on ash deposition and accurately control the concentration of ABS, based on a typical 600 MW utility boiler, pulverized ABS and fly ash were mixed thoroughly at a ratio of 1:70, which was also used in the works of other researchers [19]. After the probe surface temperature stabilized, the mixtures of ash and ABS were continuously and steadily added to the pipeline by the ash feeder. The experimental process was divided into three stages: deposition stage for 120 min, reheating stage for 60 min, followed by cooling stage for 30 min. In the deposition and cooling stage, the deposition surface temperature was maintained at 200 °C. During the reheating stage, the temperatures of the deposition surface were reheated to 335 °C, 365 °C, 385 °C, and 430 °C. In this work, the "reheat temperature" referred to the temperature of the probe head surface when the heating element heated the probe head during the reheating stage. In case 1, ash deposition was not reheated, while in case 2, the ash deposition was reheated only by hot air. Fig. 3 shows the reheat temperatures of the probe head surface during the reheating stage. The maximum deviations from the set value in cases 2~6 were 0.99%, 1.20%, 1.06%, 0.66%, 1.85%, respectively. The mixture of ash and ABS was added in the deposition and reheating stage, but the ash feeder was stopped during the cooling stage. The fly ash used in the experiment was collected from the electrostatic precipitator of a power plant in Zhejiang Province, China. The average particle size of the fly ash is 24.53um, and the chemical composition of the fly ash is listed in Table 2.

Table 1
Experimental conditions.

Case	Case 1	Case 2	Case3	Case 4	Case 5	Case 6
Temperature of the flue gas (°C)	325					
Temperature of the deposition surface (°C)	200					
Gas velocity in the DTF (m/s)	9.2					
Feeding rate (kg/h)	2.62					
Blending rate (Ash:ABS, wt)	70:1					
Reheat temperature (°C)	/	320	335	365	385	430

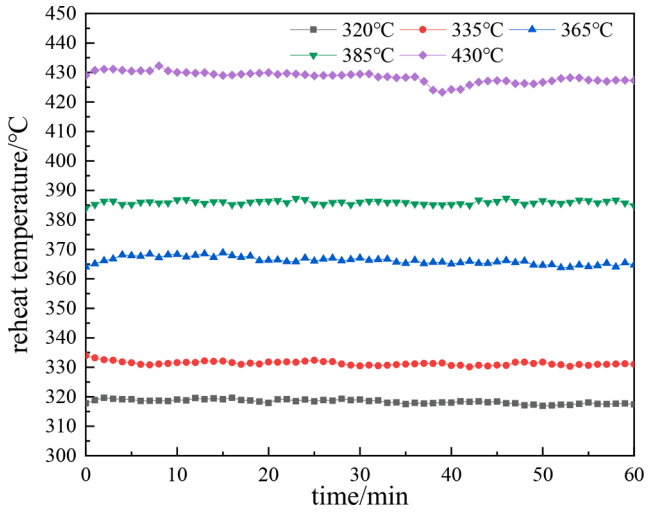

Fig. 3. Reheat temperatures of the probe head surface during the reheating stage.

2.4. Analysis methods

After the test, ash deposition was collected and ground into powder. The microstructure of the ash deposition samples was observed by a scanning electron microscope (SEM, Hitachi S-3700N), and the elemental composition was analyzed by Energy Dispersive X-Ray Spectroscopy (EDX). X-ray diffraction (XRD, PANalytical B.V. X-pert Powder) was applied to analyze the mineral composition of ash deposition samples. The weight loss was analyzed in a thermal gravimetric analyzer (TGA, Mettler TGA/DSC3+) under 100% N_2 conditions to determine the type of ammonium compounds that remained in the ash deposition.

3. Results and discussion

3.1. Visual evaluation of ash deposition

Fig. 4 shows the ash deposition on the deposition surface of the probe head after the test. By comparison, it could be seen that in the deposition condition, 320 °C and 335 °C conditions, there were many depositions on the surface of the probe, and the deposition surface was very rough. When the ash deposition was reheated only by hot air or the reheat temperature was low, there were no cleaning effects on the ash already formed. With the increase of the reheat temperature, under the conditions of 365 °C, 385 °C and 430 °C, the ash deposition on the surface of the probe head was obviously reduced, and the metal surface of the probe head could be seen from the picture, which was not seen in the first three cases. Moreover, as the reheat temperature increased, the metal surface area expanded, which meant that when the reheat temperature exceeded the decomposition temperature of ABS, some ash depositions formed before would be cleaned. The higher the reheat temperature was, the more noticeable this effect was. Because the liquid ABS had a strong viscosity. After ABS was added to the pipeline, it was heated and melted by the hot flue gas. Liquid ABS in the flue gas played the role of binder between the probe surface and the fly ash and among the ash particles. The ABS and ash mixture was tightly deposited on the deposition surface, forming the ash deposition. When the reheat temperature exceeded the decomposition temperature of ABS, ABS would decompose so that the cohesive force would weaken, and the dense ash deposition would become loose. Under the flushing of flue gas, the loose deposition would be taken away. When collecting samples, the samples in the first three cases were difficult to scrape, for the ash deposition was tightly stuck to the probe surface, while the samples in the last three cases were easy to scrape.

Table 2
The chemical composition of the fly ash.

SiO_2	Al_2O_3	Fe_2O_3	CaO	K_2O	TiO_2	MgO	SO_3	SrO	Na_2O	P_2O_5	BaO	MnO
34.91	27.86	14.85	14.04	1.73	1.70	1.33	1.22	0.73	0.60	0.23	0.20	0.19

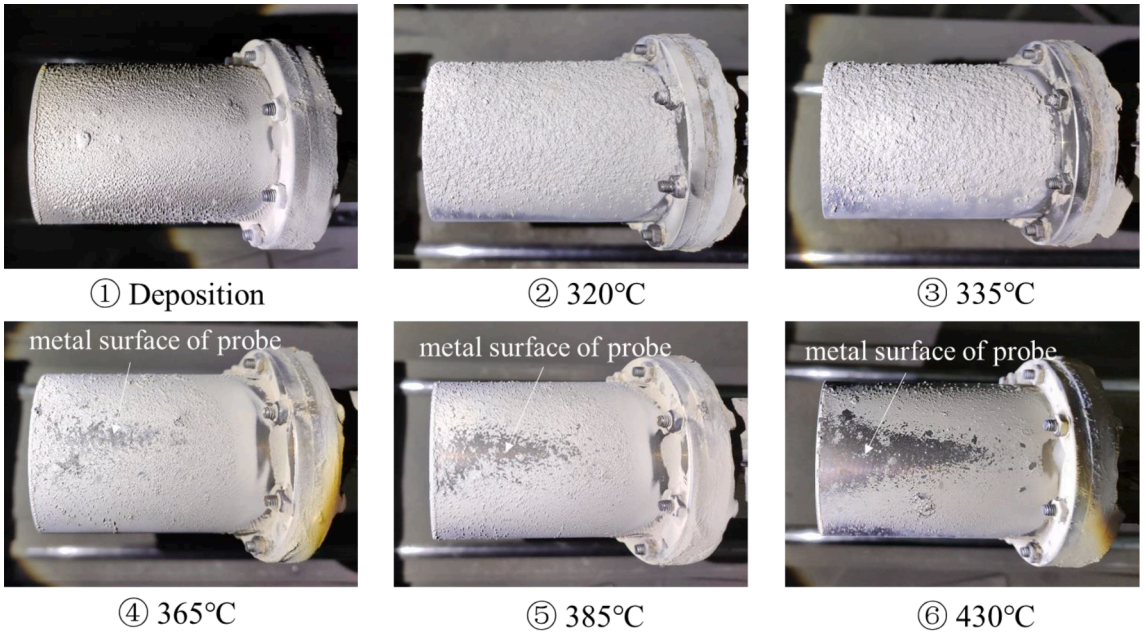

Fig. 4. The photos of ash deposition.

3.2. Microstructure of ash deposition

Fig. 5 illustrates a typical SEM image of the ash deposition. The EDX was used to analyze four spots in Fig. 5, and the results are listed in Table 3. Spots a and b represented the junction of the ash particles, and spots c and d referred to the ash particles. The S element content of spots a, b, c, and d were 7.12, 6.24, 1.00, and 0.67, respectively. The content of the S element on the surface of the ash particles was minimal, while the content of S at the particle connection was very high. Moreover, only ABS was introduced into the test system. It could be inferred that the ABS was conducive to the agglomeration of ash particles. Melted ABS would form a liquid bridge force between particles, causing mutual adherence among particles, forming ash deposition on the lower temperature surface.

SEM was applied to observe the microstructure of powder samples under all conditions and fly ash at 800X. The results are shown in Fig. 6. Fig. 6① shows the microstructure of fly ash before the test. The ash particles were dispersed, and there was no adhesion between particles. The fly ash was dominated by small and medium-sized ash particles, with a small number of large-particle ash. Compared with the fly ash, the agglomeration of ash particles was very serious in the deposition case, forming a tight microstructure. The main form of agglomeration was that fine particles were absorbed by larger particles and mutual adsorption between small particles. And the latter occupied the majority, as shown in Fig. 6②. When the deposition surface was reheated, the ash agglomeration was significantly reduced. The agglomeration became lighter as the reheat temperature increased, which may be correlated with the sample's ABS content. Fig. 6③-⑤ illustrates that although there was also aggregation in cases 320 °C, 335 °C, and 365 °C, it was much lighter than in the deposition case. When it came to cases 385 °C and 430 °C, there was almost no agglomeration among the ash particles, and the particles were dispersed, similar to the fly ash image. The particles that stick together in Fig. 6 are reduced obviously. Reheating was very effective in weakening the cohesion between the ash particles for the decomposition of ABS. Moreover, it could be seen that there were almost no large ash particles in the deposition sample or reheated sample. They were dominated by small and medium-sized particles, which indicated that small and medium-sized particles were more prone to deposit.

3.3. Heat flux through the probe

Fig. 7 shows the relative heat flux under different cases. In the figure, q/q_0 represents the relative heat flux, where q_0 is the initial heat flux, and q is the heat flux through the deposition surface of the probe head. The first 120 min was the deposition stage. The ABS and ash blend deposited on the deposition surface, causing the relative heat flux to decrease. Followed by a 60 min reheating stage, the probe surface temperature was reheated to the set value. And then, the probe surface temperature was cooled to 200 °C for 30 min. It was used to compare the change of the relative heat flux before and after reheating to judge the deposition on the probe surface.

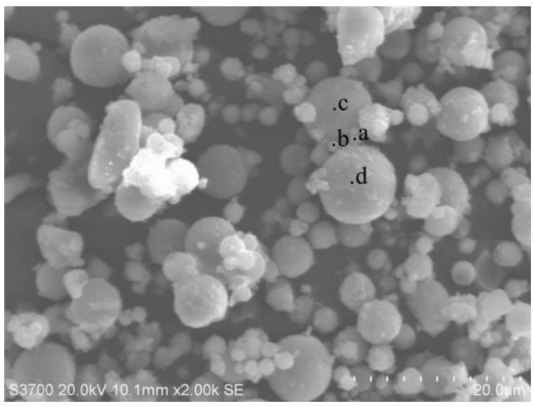

Fig. 5. A typical SEM image of the ash deposition.

It could be seen from Fig. 7 that within 20 min of starting deposition, the relative heat flux density decreased fast and then decreased slowly. It was stable at 110~120 min. When stable, the relative heat flux of cases 1~6 were about 0.881, 0.899, 0.888, 0.887, 0.852 and 0.842, respectively. After 60 min of reheating, the probe was cooled to deposition temperature with relative heat fluxes of 0.941, 0.930, 0.986, 0.997 and 0.997 for cases 2~6, respectively. It illustrated that the relative heat flux was obviously improved after reheating. When the reheat temperature was 365 °C, the relative heat flux increased to 0.986, which almost eliminated the influence of fouling.

3.4. XRD analysis

To investigate the effects of reheat temperatures on the mineral composition of ash deposition, XRD was used to analyze the mineralogy of the powder samples. The results are shown in Fig. 8. The detailed mineral composition is listed in Table 4. The quartz and mullite were the main components in all samples. Calcite ($CaCO_3$), CaO, tschermigite, and $(NH_4)_3Al(SO_4)_3$ were found in the fly ash. Nevertheless, after adding ABS, the diffraction peaks of Calcite ($CaCO_3$) and CaO disappeared. In consideration of $CaSO_4$ found in other samples, it could be inferred that the following reactions occurred:

$$CaCO_3 + NH_4HSO_4 \rightarrow CaSO_4 + NH_3 + CO_2 + H_2O \quad (10)$$

$$CaO + NH_4HSO_4 \rightarrow CaSO_4 + NH_3 + H_2O \quad (11)$$

NH_4HSO_4 was only found in deposition condition, which attributed to the decomposition of ABS under high temperature in cases 2~6. Part of NH_4HSO_4 would be decomposed in the flue gas, generating NH_3, which would react with NH_4HSO_4 to product $(NH_4)_2SO_4$, as shown in formulas (12)~(14). For the highest reheat temperature in case 6, $(NH_4)_2SO_4$ was completely decomposed according to formulas (12), (13) and (15). Godovikovite ($NH_4Al(SO_4)_2$) was created in two ways: (1) dehydration of tschermigite and (2) high-temperature reaction of Al_2O_3 and $(NH_4)_3Al(SO_4)_3$, and the reaction formulas were shown in formula (16) and (17) [20,21].

$$2NH_4HSO_4 \rightarrow (NH_4)_2S_2O_7 + H_2O \quad (12)$$

$$3(NH_4)_2S_2O_7 \rightarrow 2NH_3 + 6SO_2 + 2\,N_2 + 9H_2O \quad (13)$$

$$NH_4HSO_4 + NH_3 \rightarrow (NH_4)_2SO_4 \quad (14)$$

$$(NH_4)_2SO_4 \rightarrow NH_4HSO_4 + NH_3 \quad (15)$$

$$NH_4Al(SO_4)_2{\cdot}12H_2O \rightarrow NH_4Al(SO_4)_2 + 12H_2O \quad (16)$$

$$4(NH_4)_3Al(SO_4)_3 + Al_2O_3 \rightarrow 6NH_4Al(SO_4)_2 + 6NH_3 + 3H_2O \quad (17)$$

3.5. Weight loss characteristic

Fig. 9 shows the temperature curve, weight loss curve, and derivative thermogravimetry (DTG) curves of the powder samples by TGA. The dash-dot line is the weight loss curve, and the solid line is the DTG curve in Fig. 9. The temperature of TGA was set based on the decomposition temperature of ABS and AS and the temperature settings of Wang et al. [8]. The temperature was increased from 50 °C to 1000 °C at the rate of 15 °C·min^{-1} and held at 500 °C and 800 °C for 30 min, respectively. There are five prominent weight loss peaks in Fig. 9. Table 5 lists the characteristic temperature of weight loss peaks, the weight loss of every peak, and the final weight loss.

Due to the existence of external and crystal water, in the temperature

Table 3
The EDX results of the four spots. (wt.%).

	O	Na	Mg	Al	Si	S	K	Ca	Ti	Fe	Cu
a	35.15	0.21	0.96	8.77	16.06	**7.12**	0.35	22.39	0.95	6.94	1.1
b	49.88	0.35	0.99	8.52	15.08	**6.24**	0.24	14.19	0.56	3.54	0.41
c	40.4	–	0.73	14.26	21.21	**1.00**	–	19.5	0.19	2.18	0.52
d	45.93	–	1.81	11.61	21.35	**0.67**	0.12	14.02	1.03	3.09	0.37

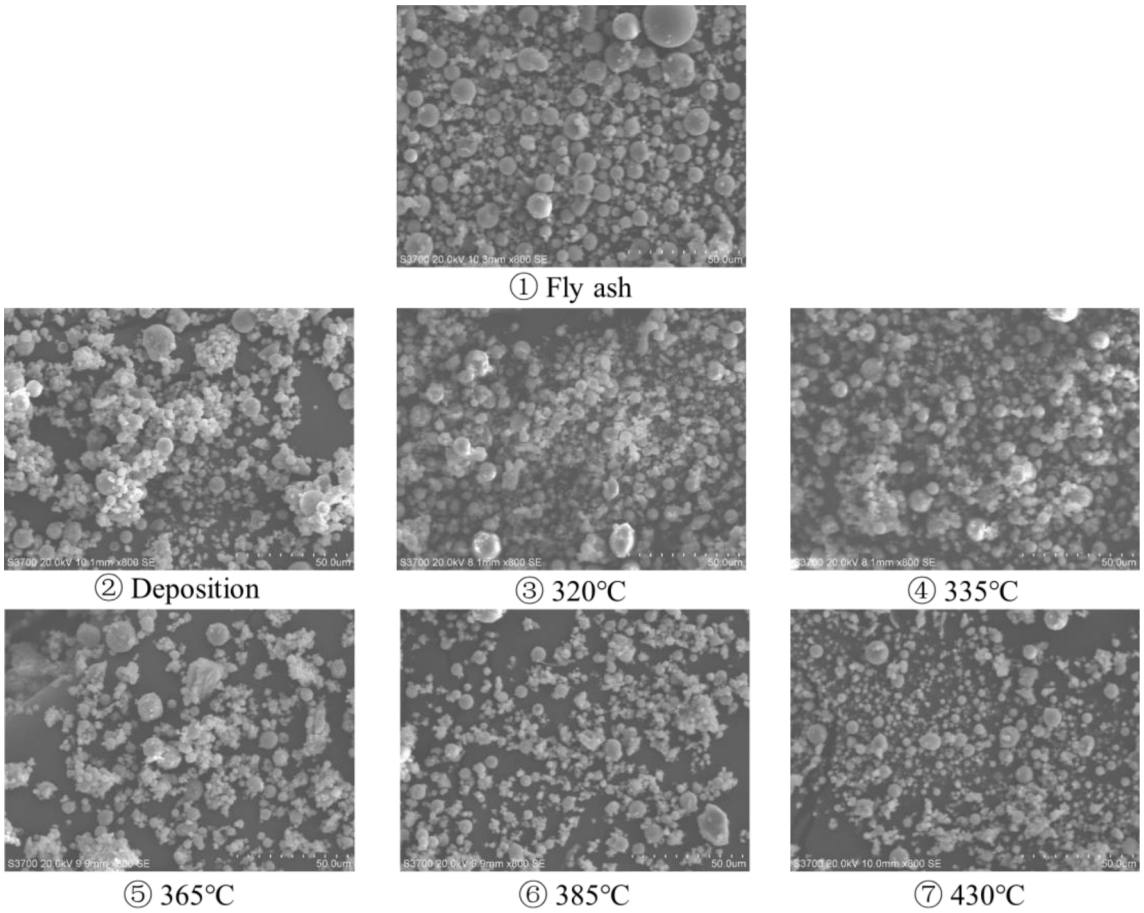

Fig. 6. The microstructure of ash deposition.

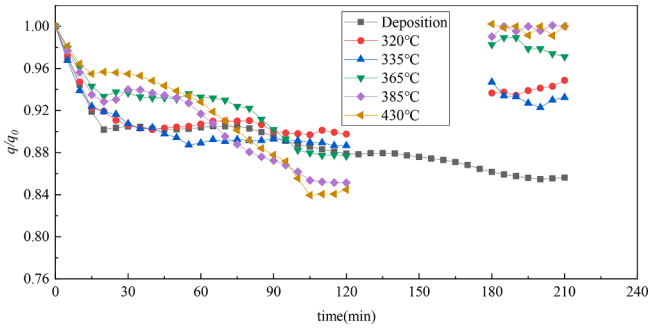

Fig. 7. Relative heat flux through the deposition probe.

range of 50~200 °C, the first weight loss peak appeared. For the difference in environmental moisture during the experiment and TGA, which was inevitable, the weight loss of the samples at Peak ① was quite different. However, this would not affect the experiment results because this paper mainly studies the effect of reheat on ABS. So this work mainly focused on the weight loss peaks ② ~ ⑤.

For deposition condition, the characteristic temperature of peak ② was 351.12 °C. According to the reference [20,22], $(NH_4)_2SO_4$ begins to decompose in 213~308 °C, and ABS begins to decompose in the range of 308 ~ 330 °C. When the temperature exceeds 300 °C, tschermigite will be completely dehydrated, so formulas (12), (15) and (16) maybe contribute to the weight loss at peak ②. The characteristic temperature of peak ③ was 392.75 °C. NH_4HSO_4 reached the maximum decomposition rate (formula (12)) at this peak. And the characteristic temperature of peak ④ was 450.72 °C. At this peak, $(NH_4)_2S_2O_7$ reached the maximum decomposition rate (formula (13)) [15,22]. So the appearance of peaks ③ and ④ and the partial weight loss of peak ② were due to the decomposition of ABS and AS. The decomposition temperature of godovikovite is above 541 °C [20], and the characteristic temperature of peak ⑤ is 655.55 °C. The decomposition of godovikovite led to the weight loss at peak ⑤, corresponding to formula (18).

$$2NH_4Al(SO_4)_2 \rightarrow Al_2(SO_4)_3 + 2NH_3 + SO_3 + H_2O \quad (18)$$

The analysis of peaks ② to ⑤ was also applicable to cases 2~6. Only the characteristic temperature of each peak was slightly different. At the same time, it was found that the third and fourth peaks in case 4 were very small, and the peaks in case 5 and case 6 almost disappeared, which

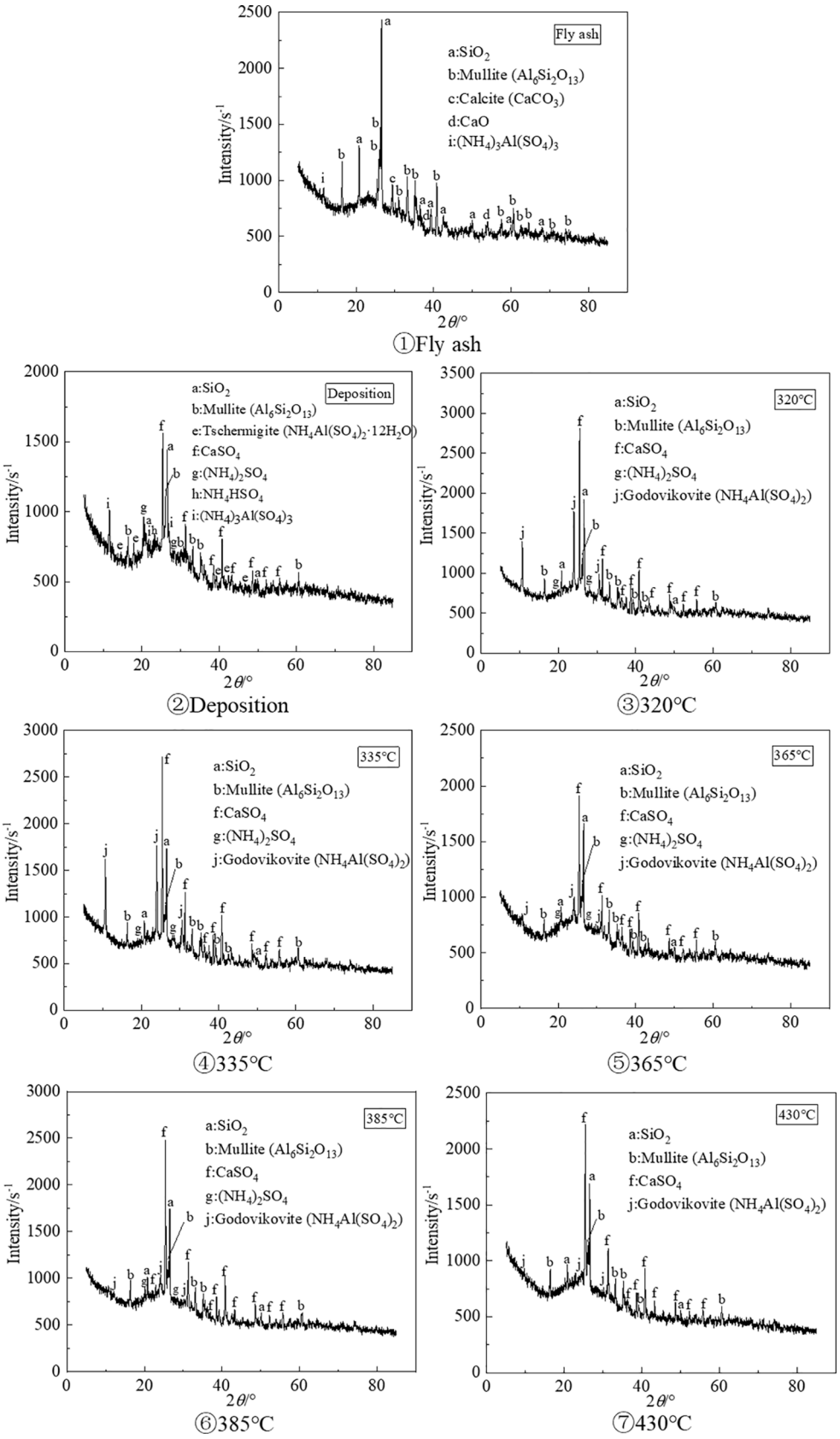

Fig. 8. XRD patterns of ash deposition samples.

Table 4
Mineral composition in the ash deposition.

Sample		Mineral composition
Fly ash		Quartz (SiO_2), Mullite ($Al_6Si_2O_{13}$), Calcite ($CaCO_3$), CaO, $(NH_4)_3Al(SO_4)_3$
Case 1	Deposition	Quartz (SiO_2), Mullite ($Al_6Si_2O_{13}$), Tschermigite ($NH_4Al(SO_4)_2{\cdot}12H_2O$), $CaSO_4$, $(NH_4)_2SO_4$, NH_4HSO_4, $(NH_4)_3Al(SO_4)_3$
Case 2	320 °C	Quartz (SiO_2), Mullite ($Al_6Si_2O_{13}$), $CaSO_4$, $(NH_4)_2SO_4$, Godovikovite ($NH_4Al(SO_4)_2$)
Case 3	335 °C	Quartz (SiO_2), Mullite ($Al_6Si_2O_{13}$), $CaSO_4$, $(NH_4)_2SO_4$, Godovikovite ($NH_4Al(SO_4)_2$)
Case 4	365 °C	Quartz (SiO_2), Mullite ($Al_6Si_2O_{13}$), $CaSO_4$, $(NH_4)_2SO_4$, Godovikovite ($NH_4Al(SO_4)_2$)
Case 5	385 °C	Quartz (SiO_2), Mullite ($Al_6Si_2O_{13}$), $CaSO_4$, $(NH_4)_2SO_4$, Godovikovite ($NH_4Al(SO_4)_2$)
Case 6	430 °C	Quartz (SiO_2), Mullite ($Al_6Si_2O_{13}$), $CaSO_4$, Godovikovite ($NH_4Al(SO_4)_2$)

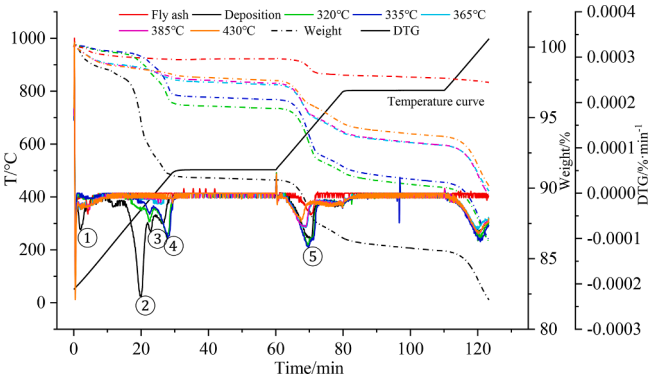

Fig. 9. Weight loss curve of the ash deposition.

meant that ABS and AS were almost wholly decomposed under cases 4~6. In cases 2~6, the total weight loss at peaks ③ and ④ was 2.80%, 2.59%, 0.84%, 0.67% and 0, respectively. Reheating had a significant influence on the decomposition of ABS. In the range of 800~1000 °C, there was also a weight loss peak, which should be the decomposition of some sulfates formed after adding ABS.

4. Conclusions

In this work, the effects of reheat temperatures on the characteristics of ash deposition were studied with a self-reheating probe, which was not studied in previous work. The following conclusions were drawn from this work.

(1) From the image of the deposition surface after the test, it can be seen that when the deposition surface is not reheated or the reheat temperature is low, a lot of ash deposition with a rough surface sticks to the deposition surface. When the reheat temperature exceeds 365 °C, the ash deposition is significantly reduced, and the metal surface of the probe head can be seen. The area of the metal surface increases with increasing reheat temperature.

(2) The SEM-EDX results show that the viscous ABS is the main reason for the agglomeration of fly ash and the formation of ash deposition. Moreover, small-sized ash particles are more likely to agglomerate. Reheating can reduce the agglomeration of particles by weakening the cohesive force of ABS between particles. The higher the reheat temperature, the more dispersed the particles are.

(3) The relative heat flux through the probe is stable at about 110~120 min, with a value of about 0.881. After reheating, the relative heat flux has been significantly improved, 0.941, 0.930, 0.986, 0.997 and 0.997 for cases 2~6, respectively. When the reheat temperature exceeds 365 °C, the impact of ash deposition is basically eliminated.

(4) XRD and TGA results show that the main mineral composition of ash deposition is Quartz, Mullite, Tschermigite, $CaSO_4$, $(NH_4)_2SO_4$, NH_4HSO_4 and Godovikovite. After reheating stage, $(NH_4)_2SO_4$ and NH_4HSO_4 will decompose. When the reheat temperature is 365 °C, only a tiny fraction of ABS and AS remain. When the reheat temperature exceeds 385 °C, the ABS and AS in the ash are almost entirely decomposed. The reheating method can eliminate ash deposition formed by decomposing the ABS to weaken particle-to-deposition surface adhesion and particle-to-particle adhesion.

(5) The above results show that when the reheat temperature exceeds 365 °C, the probe head can expose more metal surface, particle agglomeration in the microstructure is significantly reduced, the relative heat flux is increased, and the ABS and AS content in the ash deposition becomes minimal. So 365 °C can be chosen as a typical reheat temperature in engineering applications. Although it is better to raise the reheat temperature, it will result in additional heat losses or auxiliary power. Based on the experimental results, two methods for cleaning the ash deposition already formed on the air preheater are proposed. ①Add a flue gas bypass before the air preheater. When cleaning the air preheater, flue gas from the flue gas bypass with a temperature exceeding 365 °C can be used to heat the air preheater for more than 1 h. ②Add electric heating wires inside the heat exchange plates of the air preheater. When the air preheater needs to be cleaned, the electric heating wires raise the surface temperature of the air preheater to 365 °C and maintain that temperature for more than 1 h.

Table 5
Characteristic temperature and weight loss of the ash deposition.

	Fly ash	Case 1 Deposition	Case 2 320 °C	Case 3 335 °C	Case 4 365 °C	Case 5 385 °C	Case 6 430 °C
				Characteristic temperature (°C)			
①	109.01	78.39	130.04	132.11	83.97	116.63	85.57
②	–	351.12	–	–	–	–	–
③	–	392.75	387.97	389.58	–	–	–
④	–	450.72	470.42	469.79	439.28	438.80	–
⑤	653.34	655.55	643.62	645.95	634.89	635.20	615.16
				Weight loss (%)			
①	0.46	1.50	0.29	0.24	1.09	1.18	1.25
②	–	5.38	–	–	–	–	–
③	–	0.99	0.88	0.56	–	–	–
④	–	1.17	1.92	2.03	0.84	0.67	–
⑤	1.00	4.38	4.90	5.12	3.68	3.78	3.32
Final	2.51	17.92	13.81	13.68	10.21	10.52	9.84

CRediT authorship contribution statement

Yuguo Ni: Methodology, Software, Validation, Formal analysis, Investigation, Data curation, Writing – original draft. **Yan Rong:** Methodology, Software, Validation, Formal analysis, Investigation. **Xinfeng Yu:** Methodology, Software, Validation, Formal analysis, Investigation. **Shengyao Huang:** Methodology, Software, Validation, Formal analysis, Investigation. **Xue Xue:** Methodology, Software, Validation, Formal analysis, Investigation. **Hao Zhou:** Conceptualization, Writing – review & editing, Visualization, Supervision, Project administration, Funding acquisition, Formal analysis, Investigation.

Declaration of Competing Interest

The authors declare that they have no known competing financial interests or personal relationships that could have appeared to influence the work reported in this paper.

Acknowledgement

This work was supported by the National Science Fund for Distinguished Young Scholars (No. 51825605).

References

[1] Ul Hai I, Sher F, Yaqoob A, Liu H. Assessment of biomass energy potential for SRC willow woodchips in a pilot scale bubbling fluidized bed gasifier. Fuel 2019;258:116143.
[2] Razzaq L, Farooq M, Mujtaba MA, Sher F, Farhan M, Hassan MT, et al. Modeling viscosity and density of ethanoldiesel- biodiesel ternary blends for sustainable environment. Sustainability 2020;12(12):5186.
[3] Al-Shara NK, Sher F, Iqbal SZ, Sajid Z, Chen GZ. Electrochemical study of different membrane materials for the fabrication of stable, reproducible and reusable reference electrode. J Energy Chem 2020;49:33–41.
[4] Al-Shara NK, Sher F, Yaqoob A, Chen GZ. Electrochemical investigation of novel reference electrode Ni/Ni(OH)₂ in comparison with silver and platinum inert quasireference electrodes for electrolysis in eutectic molten hydroxide. Int J Hydrogen Energy 2019;44:27224–36.
[5] Schreifels JJ, Wang SX, Hao JM. Design and operational considerations for selective catalytic reduction technologies at coal-fired boilers. Front Energy 2012;6(1):98–105.
[6] Zhou C, Zhang L, Deng Y, Ma S-C. Research progress on ammonium bisulfate formation and control in the process of selective catalytic reduction. Environ Prog Sustainable Energy 2016;35(6):1664–72.
[7] Matsuda S, Kamo T, Kato A, Nakajima F, Kumura T, Kuroda H. Deposition of ammonium bisulfate in the selective catalytic reduction of nitrogen oxides with ammonia. Ind Eng Chem Prod Res Dev 1982;21:48–52.
[8] Wang L, Bu Y, Tang C, Lv C, Chen X, Che D. Study on the formation process of low-temperature ash deposition induced by ammonium bisulfate in pulverized coal-fired boiler. Asia-Pac J Chem Eng 2020;15:e2389.
[9] Wright TL, DeLallo MR. Increased SO_3 and ammonia slip from SCR: balancing air heater deposits, ammonia in effluent discharge, and SO_3 plume. Pennsylvania: National Energy Technology Laboratory; 2002.
[10] Muzio L, Bogseth S, Himes R, Chien Y-C, Dunn-Rankin D. Ammonium bisulfate formation and reduced load SCR operation. Fuel 2017;206:180–9.
[11] Menasha J, Dunn-Rankin D, Muzio L, Stallings J. Ammonium bisulfate formation temperature in a bench-scale single-channel air preheater. Fuel 2011;90:2445–53.
[12] Sarunac N. Power 101: Improving the performance of boiler auxiliaries, part ii. Coal Power 2011.
[13] Zhou LS, Ming DZ, Li ZX, Li HP. The mechanism of thermal decomposition for ammonium sulfate and ammonium bisulfate via addition of ferric oxide. Adv Mater Res 2013;803:68–71.
[14] Li P, Liu QY, Liu ZY. Behaviors of NH_4HSO_4 in SCR of NO by NH_3 over different cokes. Chem Eng J 2012;181–182:169–73.
[15] Zhu Z, Niu H, Liu Z, Liu S. Decomposition and reactivity of NH_4HSO_4 on V_2O_5/AC catalysts used for NO reduction with ammonia. J Catal 2000;195:268–78.
[16] Vuthaluru HB, French DH. Investigations into the air heater ash deposit formation in large scale pulverised coal fired boiler. Fuel 2015;140:27–33.
[17] Srivastava RK, Miller CA, Erickson C, Jambhekar R. Emissions of sulfur trioxide from coal-fired power plants. J Air Waste Manag Assoc 2004;54:750–62.
[18] Zhang J, Zhou H, Bai Z, Cen K. Experimental investigation of the effect of two additives on the characteristics of low-temperature fouling with an in-situ measurement technique. Appl Therm Eng 2020;164:114445.
[19] Liang DK. Experimental research on the effects to flue ash particles characteristics of NH_4HSO_4 generating during the denitrification process. Shandong, China: Shandong University; 2014.
[20] Tong QQ. Research on preparation of aluminum oxide and flocculant from bauxite tailing. Hunan, China: Central South University; 2013.
[21] Zhou GB, Peng TJ, Sun HJ, et al. The products transformation and formation mechanism in the roasting process of high Ti-bearing blast furnace slag with ammonium sulfate. Acta Petrol Mineral 2013;32(6):893–8.
[22] Fan YZ, Cao FH. Thermal decomposition kinetics of ammonium sulfate. J Chem Eng Chin Univ 2011;25(2):341–9.